Formation of Guided Cherenkov Radiation in Silicon-Based Nanocomposites

Aycan Yurtsever, Martin Couillard, and David A. Muller
School of Applied and Engineering Physics, Cornell University, Ithaca, New York 14850, USA
(Received 22 August 2007; published 29 May 2008)

We use a monochromated 200 keV electron beam as a nanometer-resolution probe of the photonic density of states in bulk and nanoparticle Si/SiO_2 systems, observing infrared to ultraviolet waveguided Cherenkov modes in Si slabs, but none in SiO_2. While isolated Si nanoparticles are too small to support Cherenkov radiation, we find high densities of Si nanoparticles in SiO_2 support a damped form of the radiation, with the modes determined by the effective medium of the Si/SiO_2 mixture. The guided nature of the radiation is confirmed by the presence of a thickness-dependent cutoff.

DOI: 10.1103/PhysRevLett.100.217402 PACS numbers: 78.67.Bf, 41.60.Bq, 42.82.Et, 79.20.Uv

Energy loss mechanisms of fast electrons as a result of interaction with matter have been widely studied and used as means to investigate material properties at the atomic scale [1]. Among the relatively well-known loss mechanisms are the excitation of core level electrons, excitation of bulk and surface/interface plasmons and excitation of single valence electrons. In addition to these losses, a semirelativistic electron traveling faster than the speed of light in a dense macroscopic material may suffer an additional energy loss due to Cherenkov radiation (CR) [2,3]. When this radiation is confined in a waveguided structure, the nature of the loss changes from a continuum to a series of peaks in the electron energy loss (EEL) spectrum, which maps the structure's photonic density of states [4]. Observations of such modes by fast electrons, based on momentum-resolved experiments in translationally invariant systems, have been reported [5,6].

The theoretical formulation of CR in homogeneous slabs is well understood [7]. However, its formation in packed, inhomogeneous nanoparticle systems is less clear. In particular, it is not clear if the particles will radiate when the nanoparticle sizes are much smaller than the characteristic formation lengths. Further, under what conditions is it appropriate to describe the whole composite system with a single dielectric function, as an effective medium, for the purpose of energy loss of a fast electron [8]?

In this Letter, we use EEL spectroscopy with a 200 keV incident electron energy to study the formation of CR and waveguided modes, both experimentally and theoretically, in the 0.7–3.4 eV (infrared-ultraviolet) range with 100 meV energy resolution. First, we study homogeneous crystalline Si (c-Si) slabs to demonstrate that our experimental conditions and relativistic local dielectric theory are sufficient to observe and understand the guided modes in the EELS. Then, we use Si nanoparticles ($\sim$4 nm in size) embedded in SiO_2 slabs, a materials system with potential technological applications, including as a gain medium in photonic circuitry [9], to explore the conditions for CR and guided modes in inhomogeneous media, and to what extent EELS can be used as a nm-resolution probe of photonic materials and devices. In addition to its fundamental importance, this is critical for several proposed applications of monochromated fast electrons including their influence on the band gap measurements [10] and on the study of nanoparticles. Furthermore, the high thickness sensitivities of the guided modes could either be used for very accurate slab thickness measurements or alternatively for indirect measurement of the dielectric functions of embedded nanoparticles.

The formation of CR and its ability to probe the photonic density of states can be qualitatively understood in the "virtual photon" picture, which maps the fields of a high velocity electron to the fields of an electromagnetic pulse [11]. In the far field, the fields vary within a characteristic time $\Delta t = b/\gamma v$, where $\gamma = [1 - (v/c)^2]^{-1/2}$, v is the speed of electron (in our case $v = 0.69c$), c the speed of light in vacuum, and b the impact parameter. Their frequency spectrum $S(\omega)$ has a cutoff at $\Delta f \sim 2\pi/\Delta t$. One way to convert virtual photons into real radiation is by CR. As the final photonic states begin to differ from a continuum, like in the case of a waveguide medium, the frequency spectrum of the virtual photons further needs to be modified. If $D(\omega)$ is the photonic density of states, then the frequency spectrum will approximately be $\sim D(\omega)S(\omega)$, and it is this spectrum that EELS probes. Hence, a fast electron acts as a broadband "light source" that can be placed within the optical structure with angstrom spatial resolution [4].

Si nanoparticles embedded in SiO_2 were grown by plasma-enhanced chemical vapor deposition of Si-rich films that were then annealed in nitrogen at 1100 °C for 3 hours, as we detailed in Refs. [12,13]. These post-annealed samples were characterized by 3D plasmon tomography [12] and core loss (Si$L_{2,3}$ and OK edge) EELS [13], both of which showed a complete phase separation to Si nanoparticles and SiO_2. A stoichiometry of $SiO_{1.1}$ was measured by Rutherford backscattering. Experiments were carried out in a monochromated FEI Tecnai F20-ST FEG-TEM with a Gatan Tridiem 865ER imaging spectrometer. The microscope's energy resolution and sample preparation are detailed in the supplied EPAPS document [13]. Within the microscope, samples were oriented such that

the surface plane would be perpendicular, within a few mrad, to the trajectory of the incident electrons. Finally, the scattered electrons were collected with a 6.5 mrad (1.63 $Å^{-1}$) collection aperture in parallel beam incidence (for c-Si slabs) over an area of diameter 80 nm and with 10 mrad (effective) in convergent beam incidence (for $SiO_{1.1}$ films) over an area of 20 nm × 20 nm.

Experimental and theoretical data for c-Si slabs with different thicknesses are shown in Fig. 1(a), demonstrating a very good agreement. The theory is based on Kröger's relativistic local dielectric formalism [7,14], with the frequency-dependent dielectric function taken from the optical data [15]. The features in the loss spectra below ~3.4 eV (where the imaginary part of the dielectric function shows a local maximum due to a Van Hove singularity) change with thickness. As the thickness increases, more peaks begin to appear while the existing peaks shift to lower energies. This behavior can be qualitatively understood by coupling of the incident electrons to the photonic guided modes of c-Si slabs. The CR condition is satisfied within the direct bandgap of c-Si. Radiation is emitted such

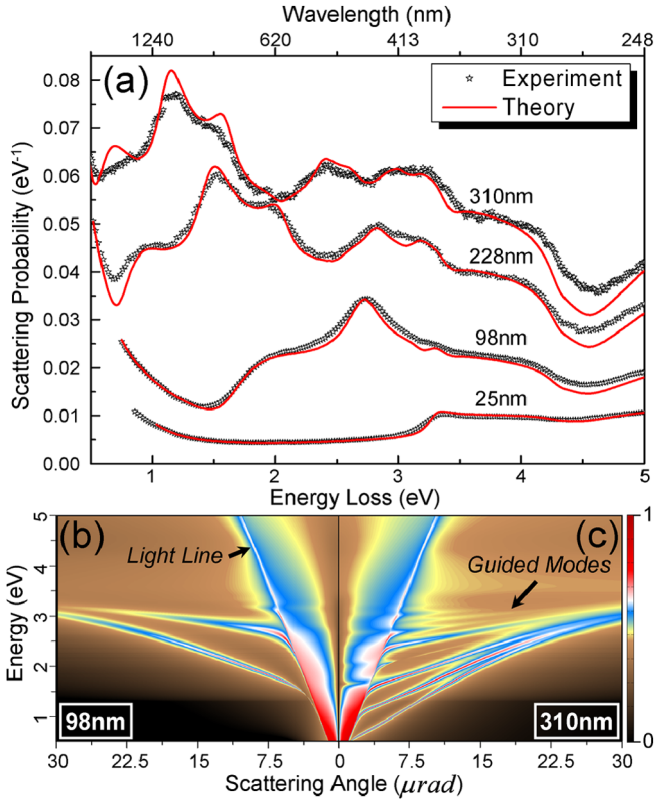

FIG. 1 (color online). (a) Experimental and theoretical spectra for different c-Si slab thicknesses for 200 keV incident electron energy. Experimental spectra were normalized to the corresponding theoretical bulk plasmon maxima at 17 eV. The top axis shows the corresponding excitation wavelengths in vacuum. A model for the zero-loss-peak (ZLP) tail is added to the theoretical spectra. The numbers correspond to the thicknesses used in the theory. (b), (c) Simulated loss images for 98 and 310 nm thick c-Si slabs, with false color log scale.

that its wave fronts form a cone with a characteristic angle of 65° (at 1 eV), satisfying the total internal reflection condition at the Si/vacuum interface. The light cannot escape the sample, but forms standing waves along the sample's normal and propagating waves along the directions parallel to the surfaces, as occurs in two-dimensional guided media. As the sample thickness increases, longer wavelength (lower energy) modes are supported, as observed in Fig. 1(a).

Figures 1(b) and 1(c) show simulated loss images, plotted as a function of both energy loss and scattering angle (wave vector). The theoretical EEL spectra in Fig. 1(a) were calculated by integrating these loss images over the scattering angle within the microscope's collection aperture. Two distinct areas in the loss images can be identified by the "light line," given by the dispersion of photons in vacuum ($\omega/k = c$). Excitations inside the light line include radiative losses as well (mostly due to the transition radiation [11]), but they do not significantly contribute to the EEL spectra at the energies and thicknesses we are interested in. Excitations outside the light line are Cherenkov losses in the form of p-polarized (magnetic field parallel to the surfaces) guided modes, with the lowest energy mode being antisymmetric. The nature of the fields of a fast electron and incident geometry allow only p-polarized modes to be excited, with alternating symmetries. Because of the rapid increase of optical absorption, all guided modes converge to the direct bandgap of c-Si at 3.4 eV. In addition, a finite absorption above the indirect bandgap at 1.1eV increases the width of the modes.

Although the formation and propagation of CR in homogeneous slabs are well understood, conditions for its formation in nanoparticle composite material systems are less clear. Propagation of light in an inhomogeneous medium can be understood by approximating the composite's dielectric function by a Maxwell-Garnett (MG) effective medium, provided the particle dimensions are much shorter than the propagating wavelengths [16]. In terms of formation of CR, however, the effective medium theories have never been used. CR is a coherent, far-field response of the medium to the passing electron. Therefore, material must extend to some degree for it to be formed [17]. The so-called formation lengths, transverse and longitudinal, are on the order of radiation wavelengths in the medium (~100 nm for Si). A single isolated nanoparticle with dimensions much smaller than the formation lengths will not support any CR. However, if a packed nanoparticle system can be treated as an effective medium in the context of "formation," it may satisfy the Cherenkov condition and radiate. In the following sections, we investigate this phenomenon in a Si-based nanocomposite material system.

The average size of Si nanoparticles in SiO_2 (np-Si/SiO_2) was measured to be ~4.2 nm with energy filtered transmission electron microscopy (TEM) [Fig. 2(a)] and tomography [12]. Average interparticle distance (center to center) was estimated to be ~8 nm.

We found most of these particles to be amorphous, with an estimated amorphous/crystalline particle ratio of ~2.3, in an agreement with previously reported values [18]. Theoretical calculations were done using the frequency-dependent, bulk dielectric constants of amorphous and crystalline Si [15], in a three-component MG approximation [19]. Si nanoparticles at these dimensions support a bulk plasmon at the macroscopic Si value of ~17 eV [Fig. 2(a)]. For our purposes, the particles are large enough to be represented by the macroscopic, homogeneous dielectric function, although quantum confinement may introduce slight modifications.

Experimental results [Fig. 2(b)] show that the strong guided modes do not exist in np-Si/SiO_2 slabs, as they existed in c-Si slabs. In addition, the scattering intensity in np-Si/SiO_2 is not a linear superposition of scattering intensities in Si and SiO_2 slabs. This observation suggests that the Si nanoparticles are not simply behaving like homogeneous c-Si in terms of formation and propagation of CR, and the host material (SiO_2) must also be taken into account. The successful use of the MG effective medium approximation in propagation of light in such media suggests that it might also be used to explain the formation of guided modes. However, the model assumes the nanoparticles are dilute enough that particle-particle interactions can be neglected. Our system may exhibit interparticle interactions in the form of surface plasmons at internal interfaces and their couplings, which have energies around ~7–9 eV, a factor of 2 higher than the energies of the guided modes. In this energy range, where the CR has damped out, the MG theory fails and more sophisticated models are needed [20]. In addition, the density and size distribution of the nanoparticles do not change with sample thickness, so contributions from the bulk and surface plasmon modes of individual nanoparticles are not expected to change with sample thickness either. Plasmons at the top and bottom planar surfaces of the specimen have energies around ~7–9 eV as well, and they will contribute weakly to the low-loss (2–3 eV) intensity in the form of a broad background that is monotonic in thickness and energy.

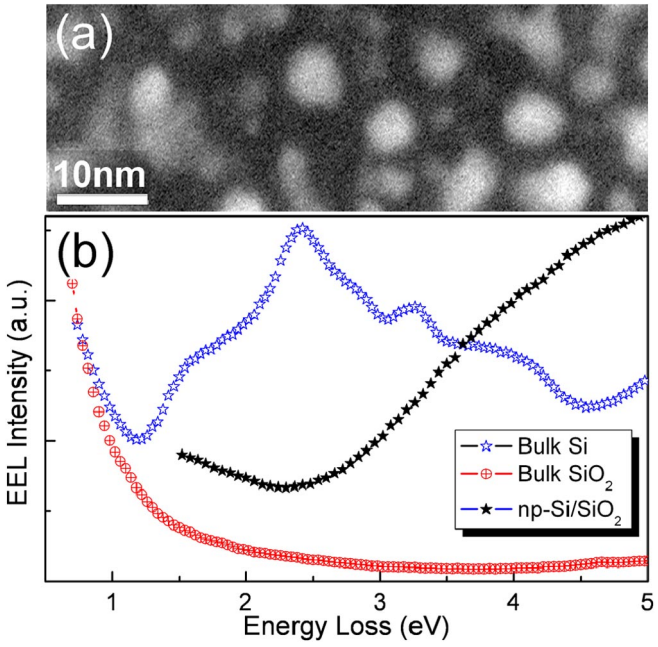

FIG. 2 (color online). (a) Energy filtered TEM image of np-Si/SiO_2, showing an average nanoparticle size of ~4 nm. (b) Experimental EELS for c-Si, thermal SiO_2, and np-Si/SiO_2 slabs at 122, ~133, and ~125 nm, respectively, demonstrating that the np-Si/SiO_2 spectrum is not a combination of bulk spectra. Spectra were normalized to the ZLP maxima.

Figure 3 shows experimental EEL spectra for np-Si/SiO_2 at different slab thicknesses together with the simulated results. At lower energies the experiment exhibits tails of the zero-loss-peak (ZLP) that are not included into the theoretical spectra for the sake of simplicity. A noticeable trend in the experimental results is the nonlinear increase of intensities in the 2.5–3.5 eV range, which also exists in the theoretical spectra as a result of appearance of an additional guided mode at ~120 nm. This abrupt change in the slope with thickness is evident in the experiment [Fig. 3(a)] between 104 and 124 nm. This change is a sign of CR, albeit with highly damped modes.

To further test the existence of CR and its confinement, the experimental and theoretical intensities between 2.5–3 eV in Fig. 3 were integrated and displayed in Fig. 4(a), together with the simulated results at the classical limit ($c \rightarrow \infty$). The classical limit does not predict any CR [21], so the intensity increase is linear with thickness. However, the relativistic curve has two distinct parts, one below ~70 nm and one above ~140 nm, in addition to the intermediate region in between. Below ~70 nm the np-Si/SiO_2 can support only one guided mode (antisymmetric p-polarized) [Fig. 4(b)]. Above the thickness of ~140 nm a second mode (symmetric p-polarized) is supported [Fig. 4(c)], resulting in a change of slope in the relativistic curve. The minimum thickness at which the second mode is allowed can be estimated by $L = \pi\hbar c/E\sqrt{\varepsilon_{\text{eff}} - 1}$, where L is the slab thickness, E the

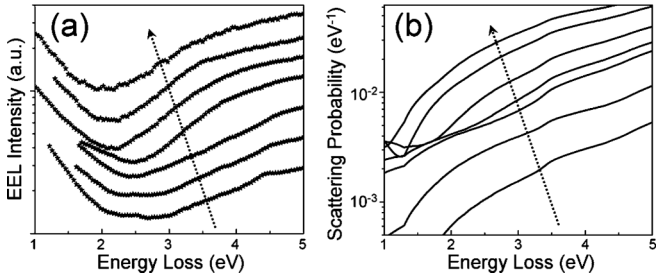

FIG. 3. (a) Experimental and (b) theoretical EEL spectra for np-Si/SiO_2. Arrows show the trend of nonlinear intensity increase in the waveguided region, indicating the presence of damped guided modes. Slab thicknesses for the spectra from bottom to top are: 16 nm, 48 nm, 104 nm, 124 nm, 175 nm, 272 nm, and 347 nm. Estimated thicknesses for experimental spectra are approximate with ≤ 20% error. Experimental spectra were normalized to the ZLP maxima.

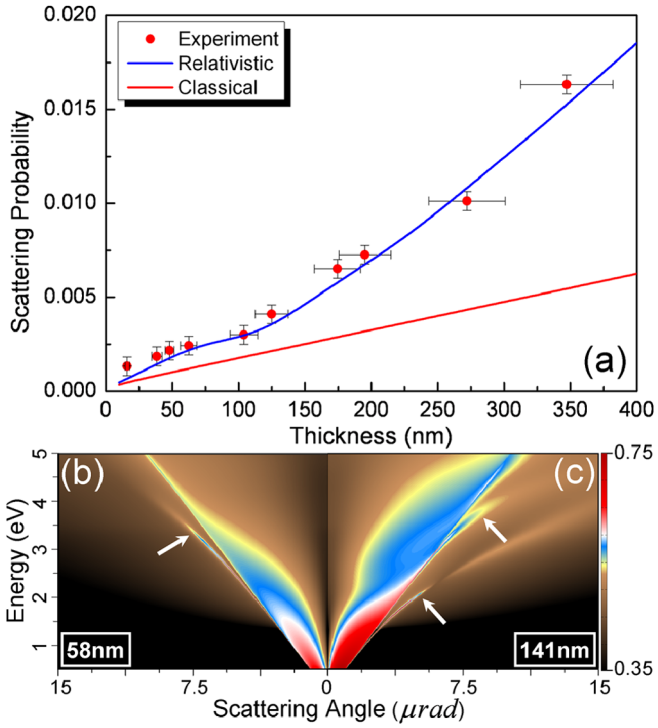

FIG. 4 (color online). (a) Integrated intensities between 2.5–3 eV of experimental and theoretical spectra in Fig. 3, together with the classical theory. Experimental data follows the relativistic curve indicating the presence of CR. In addition, the slope change at ~120 nm is due to the presence of guided modes. Experimental data is scaled to the point at 104 nm only. (b), (c) Loss images for np-Si/SiO_2 at 58 and 141 nm, respectively. The second mode is visible in (c), where they are indicated by arrows. The false color intensity scale is logarithmic.

energy, and ε_{eff} the effective dielectric constant [6]. With $E = 3$ eV and $\varepsilon_{\text{eff}} = 3.35$, L is found to be 128 nm, in close agreement with the observations. The experimental data closely follows the relativistic curve rather than the classical one. This demonstrates that np-Si/SiO_2 can indeed support CR and guided modes. This is a surprising result considering that single isolated nanoparticles at these sizes should not support any CR. Theory for a dielectric sphere [22] suggests an isolated Si particle needs a diameter larger than ~50 nm to radiate. In this Letter, we showed experimentally that small nanoparticles (~4 nm) packed together can radiate as well, but with damped intensities. This damping, in the picture of effective medium theory, can be explained by a lowered refractive index. However, a full theoretical understanding at microscopic level still needs to be developed.

Finally, we note that unannealed, as-grown $SiO_{1.1}$ shows a very similar low-energy (<5 eV) behavior to the annealed $SiO_{1.1}$, even though at ~4 nm length scale they are two very different materials; while the latter has well-separated and detectable nanoparticles, the former does not. The similar responses are expected, since these two materials have very similar refractive indexes and the MG theory is independent of the particle size, provided the long-wavelength condition is met. At higher energies (and hence shorter wavelengths) where the approximation fails, the materials show different responses [13].

In conclusion, we observed, both experimentally and theoretically, CR and waveguided modes in c-Si slabs by EELS. We also observed that Si nanoparticles embedded in SiO_2 can support CR and guided modes, but with damped intensities. In addition, the MG theory could explain the formation of the guided modes in this Si-based nanocomposite, provided the particle size and spacing are much less than the Cherenkov wavelengths.

This work is supported primarily by the National Science Foundation under Grant No. EEC-0646547. We acknowledge the use of Cornell Center for Materials Research electron microscopy facilities supported by NSF-MRSEC (DMR No. 0520404). We thank P. Tiemeijer and L. Fitting for help with the monochromator.

[1] R. F. Egerton, *Electron Energy Loss Spectroscopy in the Electron Microscope* (Plenum Press, New York, 1996).
[2] P. A. Cherenkov, Dokl. Akad. Nauk SSSR **2**, 451 (1934).
[3] I. M. Frank and I. Tamm, Dokl. Akad. Nauk SSSR **14**, 109 (1937).
[4] F. J. García de Abajo and M. Kociak, Phys. Rev. Lett. **100**, 106804 (2008).
[5] C. H. Chen and J. Silcox, Phys. Rev. Lett. **35**, 390 (1975).
[6] C. H. Chen, J. Silcox, and R. Vincent, Phys. Rev. B **12**, 64 (1975).
[7] E. Kröger, Z. Phys. **216**, 115 (1968).
[8] F. J. García de Abajo and L. A. Blanco, Phys. Rev. B **67**, 125108 (2003).
[9] L. Pavesi, L. Dal Negro, C. Mazzoleni, G. Franzo, and F. Priolo, Nature (London) **408**, 440 (2000).
[10] M. Stöger-Pollach *et al.*, Micron **37**, 396 (2006).
[11] J. D. Jackson, *Classical Electrodynamics* (Wiley, New York, 1998), 3rd ed..
[12] A. Yurtsever, M. Weyland, and D. A. Muller, Appl. Phys. Lett. **89**, 151 920 (2006).
[13] See EPAPS Document No. E-PRLTAO-100-067822 for experimental conditions and materials characterization. For more information on EPAPS, see http://www.aip.org/pubservs/epaps.html.
[14] H. Raether, *Excitations of Plasmons and Interband Transitions by Electrons* (Springer-Verlag, Berlin, 1980).
[15] E. D. Palik, *Handbook of Optical Constants* (Acedemic, Orlando, 1998).
[16] J. C. M. Garnett, Philos. Trans. R. Soc. London **203**, 385 (1904).
[17] M. S. Zolotorev and K. T. McDonald, arXiv:physics/0003096v6.
[18] F. Iacona, C. Bongiorno, C. Spinella, S. Boninelli, and F. Priolo, J. Appl. Phys. **95**, 3723 (2004).
[19] Q. Wang, D. Tian, G. Xiong, and Z. Zhou, Physica A (Amsterdam) **275**, 256 (2000).
[20] R. G. Barrera and R. Fuchs, Phys. Rev. B **52**, 3256 (1995).
[21] R. H. Ritchie, Phys. Rev. **106**, 874 (1957).
[22] F. J. García de Abajo, Phys. Rev. B **59**, 3095 (1999).